Available online at www.sciencedirect.com
ScienceDirect
Earth and Planetary Science Letters 254 (2007) 158–172
EPSL
www.elsevier.com/locate/epsl

Nb/Ta and Zr/Hf in ocean island basalts — Implications for crust–mantle differentiation and the fate of Niobium

Jörg A. Pfänder [a,*], Carsten Münker [a,b], Andreas Stracke [c,1], Klaus Mezger [a]

[a] Zentrallabor für Geochronologie (ZLG), Institut für Mineralogie, Universität Münster, Corrensstr. 24, 48149 Münster, Germany
[b] Mineralogisch-Petrologisches Institut, Universität Bonn, Poppelsdorfer Schloss, 53115 Bonn, Germany
[c] Max-Planck-Institut für Chemie, Abteilung Geochemie, Postfach 3060, 55020 Mainz, Germany

Received 20 June 2006; received in revised form 17 November 2006; accepted 17 November 2006
Available online 9 January 2007
Editor: R.W. Carlson

Abstract

Variations of high-field strength element (HFSE) ratios in terrestrial reservoirs, in particular Zr/Hf and Nb/Ta, are critical for understanding crust–mantle differentiation. Growing experimental and observational evidence shows that these ratios are fractionated during magmatic processes, despite their very similar geochemical characteristics. Here we present new high-precision Nb, Ta, Zr, Hf and Lu measurements for a variety of ocean island basalts determined by isotope dilution MC-ICPMS together with Hf isotope compositions in order to constrain OIB source characteristics and HFSE fractionation during mantle melting and crystal fractionation. Observed variations in Zr/Hf are larger than expected from fractional crystallisation alone. Partial melting of garnet and/or spinel peridotite assemblages can produce the observed range in Zr/Hf and Nb/Ta ratios, but require the presence of grossular-rich garnet, i.e. of recycled eclogite or garnet pyroxenite in the source of OIBs. This is consistent with Lu/Hf ratios that are lower in OIBs than expected from partial melting of pure garnet peridotite sources.

Nb/Ta ratios in terrestrial reservoirs can be used to place constraints on crust–mantle differentiation and mantle evolution since the Archean. The average Nb/Ta in the OIB source region (15.9 ± 0.6 (1σ)) is identical to values observed in many MORB suites, but higher than the ratio of the bulk silicate Earth (~ 14) and the estimate for the continental crust (~ 12–13). Despite the inferred presence of recycled eclogite in OIB sources, which had previously been postulated to be a potential reservoir with superchondritic Nb/Ta ratios, their Nb/Ta ratios are invariably subchondritic and therefore provide no evidence for the existence of a silicate reservoir with superchondritic Nb/Ta in the Earth's mantle, and also exclude significant contributions from core material with superchondritic Nb/Ta ratios. The complementary Nb/Ta ratios in the Earth's crust and mantle with respect to bulk silicate Earth can be explained by partial melting of amphibolite bearing slabs with bulk $D_{Nb/Ta} > 1$ during crust–mantle differentiation. As melting of subducted amphibolites was probably most intense during the Archean, major portions of the continental crust may have formed early in Earth's history. Such a model is consistent with Nb/Ta ratios in Archean rocks and with ^{142}Nd and $^{176}Hf/^{177}Hf$ evidence for early Earth differentiation.

Keywords: HFSE; Nb/Ta; Zr/Hf; OIB; crustal recycling; mantle evolution

* Corresponding author. Present adress: Institut für Geologie, Technische Universität Bergakademie Freiberg, Bernhard-von-Cotta Str. 2, 09599 Freiberg, Germany. Tel.: +49 3731 393811; fax: +49 3731 393599.
E-mail address: pfaender@tu-freiberg.de (J.A. Pfänder).
[1] Present adress: Institut für Isotopengeologie und Mineralische Rohstoffe, ETH Zürich, 8092 Zürich, Switzerland.

0012-821X/$ - see front matter © 2006 Elsevier B.V. All rights reserved.
doi:10.1016/j.epsl.2006.11.027

1. Introduction

Nb/Ta and Zr/Hf ratios in terrestrial rocks vary considerably and deviate markedly from the chondritic averages, which is in good agreement with experimentally determined mineral–melt partition coefficients for the HFSE (Nb, Ta, Zr, Hf; e.g., [1–5]). In contrast to rare earth element (REE) and Sr–Nd isotope systematics (e.g., [6–8]) and Zr/Hf and other trace element ratios (e.g., Nb/U and Ce/Pb ratios), which indicate that the Earth's mantle and continental crust are complementary geochemical reservoirs with respect to chondritic meteorites, Nb/Ta ratios in *all* silicate Earth reservoirs (Earth's mantle and crust; [9–18]; Fig. 1) are invariably subchondritic (<19.9± 0.6; [19]) and thus document a clear deficit of Nb relative to Ta and other highly incompatible trace elements in the silicate Earth. The recognition of this so-called "Nb-paradox" initiated a debate about the fate of Nb in the Earth [14,19–23]. One proposed solution is a hidden reservoir of subducted eclogitic oceanic crust with superchondritic Nb/Ta ratios [20,21] in the Earth's lowermost mantle that remained isolated from mantle convection since the Archean. Such a hidden mantle reservoir was also invoked on the basis of the apparent Nd–Hf-isotope imbalance between terrestrial samples and chondrites [24], the unradiogenic Hf-isotope compositions in Archean carbonatites and kimberlites [25] and the observed ^{142}Nd-excesses in terrestrial rocks [26]. Alternatively, the missing Nb may be hosted in the Earth's core which is supported by high-pressure partitioning experiments [27], Nb measurements in magmatic iron meteorites [22] and by systematic differences in Nb/Ta and Zr/Hf ratios between the silicate Earth, lunar and martian rocks and chondrites [19].

In order to understand the origin of the Nb depletion in the silicate Earth, it is critical to know the processes that fractionate Nb/Ta and Zr/Hf during crust–mantle differentiation. This involves resolving potential variations of Nb/Ta and Zr/Hf ratios in the mantle that originate from multiple depletion (partial melting) and enrichment (e.g. subduction and crustal recycling) events that affected the mantle throughout its history. Ratios of highly incompatible trace elements in ocean island basalts (OIBs) reflect the geochemical composition of their mantle sources and therefore do not only provide information about the distribution of the HFSE in the mantle but are also the prime targets for providing additional constraints on the possible existence of a superchondritic Nb/Ta mantle reservoir.

This study presents the first high-precision HFSE and Lu concentration data for OIBs, together with Hf-isotope ratios determined on the same samples. Observed Zr/Hf and particularly Nb/Ta variations in terrestrial rocks are small, and thus high-precision concentration data are important to resolve these variations and to improve our understanding of the behaviour of Nb/Ta and Zr/Hf during crust–mantle differentiation. These data also allow to further investigate the potential role of recycled oceanic lithosphere in the source of OIBs and to reassess the distribution of the HFSE between the Earth's mantle and crust. This, in turn, can place constraints on crust forming processes that may be responsible for the Nb/Ta ratios in the present day Earth's mantle.

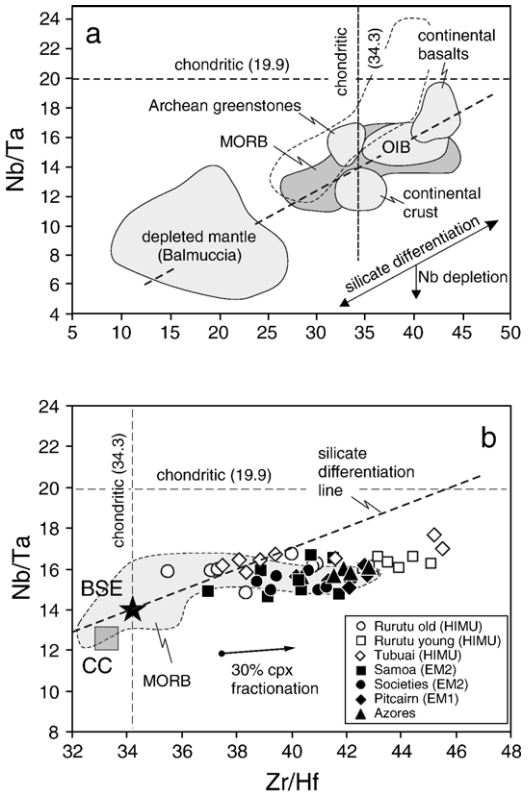

Fig. 1. (a) Nb/Ta versus Zr/Hf in major terrestrial silicate reservoirs indicating a Nb deficit with respect to Ta in the accessible silicate Earth (from [19]; dashed field: lunar samples). The silicate differentiation line (diagonal dashed line) indicates a first order coupling of Nb/Ta–Zr/Hf fractionation in terrestrial reservoirs that is in agreement with the partitioning behaviour of the HFSE. The intersection of this line with the chondritic Zr/Hf ratio defines the Nb/Ta ratio of the bulk silicate Earth (BSE). (b) Nb/Ta versus Zr/Hf in ocean island basalts. For OIBs, both ratios are decoupled, i.e. Nb/Ta remains fairly constant with variable Zr/Hf. Also shown is the field for MORB [15] as well as the average composition of the continental crust (CC, Zr/Hf and Nb/Ta from [14]). Chondritic Nb/Ta and Zr/Hf from [19]. The arrow indicates the shift in Zr/Hf and Nb/Ta that results from 30% clinopyroxene fractionation (partition coefficients see Supplementary data).

2. Samples

The ocean island basalts selected for analyses cover the entire isotopic spectrum of OIB defined by

Table 1
HFSE and Lu concentrations (μg/g) determined by isotope dilution (except Nb) and Lu–Hf isotope composition of ocean island basalts

Sample	Rock type	MgO (wt.%)	Lu	Zr	Nb	Hf	Ta	$^{176}Lu/^{177}Hf$	$^{176}Hf/^{177}Hf$	ε_{Hf}	Zr/Hf	Nb/Ta
Rurutu old (HIMU)												
RRT-32*	Basalt	6.02	0.201	124.4	22.1	3.357	1.392	0.00847	0.282956±8	+6.5	37.1	15.9
74–386	Basalt	7.24	0.246	157.9	29.3	4.230	1.837	0.00824	0.282985±13	+7.5	37.3	16.0
74–390*	Basalt	6.29	0.283	208.0	43.4	5.196	2.595	0.00773	0.282937±12	+5.8	40.0	16.7
74–396*	Basalt	7.89	0.223	190.3	38.7	4.646	2.375	0.00681	0.282972±12	+7.1	41.0	16.3
RR 01*	Basalt	7.40	0.255	188.7	42.4	4.922	2.864	0.00733	0.282930±9	+5.6	38.3	14.8
RR 03	Hawaiite	4.80	0.342	245.6	49.6	6.021	3.079	0.00805	0.282985±14	+7.5	40.8	16.1
RR 67*	Tholeiite	6.92	0.247	126.8	18.4	3.573	1.179	0.00979	0.282938±22	+5.9	35.5	15.6
RR 67 Dupl.			0.247	126.9	18.8	3.576	1.175	0.00980	0.282961±7	+6.7	35.5	16.0
Rurutu young (HIMU)												
74–394	Basanite	10.3	0.362	529.2	132.5	11.91	7.979	0.00431	0.282943±8	+6.0	44.4	16.6
RRT-60	Hawaiite	5.50	0.400	333.4	74.4	7.805	4.633	0.00726	0.283044±13	+9.6	42.7	16.1
74–392	Hawaiite	5.93	0.405	351.2	79.9	8.131	4.821	0.00706	0.283033±10	+9.2	43.2	16.6
120D	Hawaiite	6.17	0.445	391.8	86.9	9.006	5.325	0.00701	0.283081±10	+10.9	43.5	16.3
RR 20B	Hawaiite	4.34	0.435	447.6	99.7	9.920	6.137	0.00622	0.283032±12	+9.2	45.1	16.3
RR 27	Hawaiite	4.95	0.436	430.5	97.2	9.797	6.070	0.00631	0.283028±13	+9.1	43.9	16.0
RRT-15	Nephelinite	6.93	0.354	342.6	79.6	8.001	4.969	0.00628	0.283039±10	+9.5	42.8	16.0
Tubuai (HIMU)												
K109	Basanite	15.5	0.201	206.7	73.4	5.315	4.466	0.00536	0.282992±10	+7.8	38.9	16.4
5433	Basanite	6.20	0.309	278.9	96.2	6.707	5.820	0.00652	0.282977±9	+7.2	41.6	16.5
5435	Basanite	4.85	0.350	410.9	149.9	9.027	8.830	0.00550	0.282977±10	+7.3	45.5	17.0
108B	Basalt	10.9	0.293	176.1	54.4	4.621	3.300	0.00900	0.283006±7	+8.3	38.1	16.5
5434	Basalt	11.3	0.258	185.6	51.4	4.953	3.181	0.00740	0.282990±8	+7.7	37.5	16.2
5436	Basalt	9.59	0.403	194.5	65.8	4.933	3.933	0.01160	0.282990±9	+7.7	39.4	16.7
TBA36	Basalt	13.8	0.223	153.9	41.6	4.013	2.633	0.00789			38.3	15.8
110B	Nephelinite	6.99	0.409	437.2	184.9	9.674	10.48	0.00600	0.282979±9	+7.3	45.2	17.6
Azores (HIMU-EM2)												
SM0136*	Basalt	10.6	0.232	237.2	54.0	5.871	3.463	0.00560	0.283053±9	+9.9	40.4	15.6
SM0169	Basalt	8.84	0.299	338.2	59.1	8.019	3.739	0.00529	0.282854±9	+2.9	42.2	15.8
SM160501–4	Basalt	6.38	0.289	287.1	64.7	6.910	4.130	0.00594	0.283002±10	+8.1	41.6	15.7
SM0128*	Hawaiite	4.03	0.428	397.3	70.8	9.485	4.415	0.00639	0.282822±7	+1.8	41.9	16.0
SM0170*	Hawaiite	4.41	0.399	434.8	86.9	10.16	5.392	0.00556	0.282896±9	+4.4	42.8	16.1
Samoa (EM2)												
U 23 P	Basanite	11.0	0.247	266.1	65.1	6.529	3.915	0.00538	0.282923±9	+5.3	40.8	16.6
U 35 M*	Basanite	11.6	0.244	228.2	43.7	6.175	2.944	0.00561	0.282929±8	+5.6	37.0	14.8
U 13 F	Basalt	10.0	0.249	181.4	36.6	4.501	2.372	0.00786	0.283016±7	+8.6	40.3	15.4
U 24 L	Basalt	10.8	0.283	233.1	48.6	5.611	2.938	0.00715	0.282937±7	+5.9	41.5	16.5
U 39 F	Basalt	5.65	0.361	338.7	51.7	8.384	3.452	0.00611	0.282983±8	+7.5	40.4	15.0
U 43 F*	Basalt	5.34	0.362	302.8	36.1	7.731	2.470	0.00664	0.283070±8	+10.6	39.2	14.6
S46F*	Basalt	9.22	0.257	159.4	26.9	4.096	1.692	0.00890	0.282965±7	+6.8	38.9	15.9
S31P*	Hawaiite	8.96	0.224	290.5	50.4	6.956	3.418	0.00457	0.283002±7	+8.1	41.8	14.7
Society islands (EM2)												
Mu 5	Basalt	10.2	0.250	264.8	33.2	6.744	2.218	0.00526	0.282952±10	+6.4	39.3	15.0
Mu 20	Hawaiite	4.01	0.471	463.3	54.9	11.30	3.665	0.00591	0.283049±10	+9.8	41.0	15.0
Mu 29	–	–	0.264	275.6	35.0	6.677	2.323	0.00561	0.283062±10	+10.3	41.3	15.1
Ri 6	–	–	0.300	335.2	46.4	8.252	2.917	0.00515	0.283037±10	+9.4	40.6	15.9
Ri 59	–	–	0.305	313.0	38.7	7.936	2.476	0.00545	0.282994±10	+7.9	39.4	15.6
Ri 66	–	–	0.288	313.6	34.2	8.096	2.230	0.00504	0.282868±10	+3.4	38.7	15.3
Pitcairn (EM1)												
Pit89-2	Basalt	11.9	0.231	182.4	26.5	4.543	1.698	0.00721	0.282785±7	+0.5	40.2	15.6
Pit89-4	Basalt	6.42	0.331	311.9	44.3	7.545	2.871	0.00622	0.282741±9	−1.1	41.3	15.4
Pit89-10	Basalt	4.89	0.327	329.7	49.4	7.821	3.198	0.00593	0.282715±7	−2.0	42.2	15.4
Pit89-20	Hawaiite	3.71	0.501	483.7	70.7	11.49	4.686	0.00618	0.282823±9	+1.8	42.1	15.1
52DS2	Mugearite	1.72	0.601	621.5	74.5	14.57	4.610	0.00585	0.282693±9	−2.8	42.6	16.2
57DS6	Benmoreite	0.99	0.551	538.2	54.5	12.59	3.470	0.00620	0.282690±8	−2.9	42.8	15.7
USGS reference materials												

Table 1 (*continued*)

Sample	Rock type	MgO (wt.%)	Lu	Zr	Nb	Hf	Ta	$^{176}Lu/^{177}Hf$	$^{176}Hf/^{177}Hf$	ε_{Hf}	Zr/Hf	Nb/Ta
BHVO-1	–	–	0.2788	166.1	17.06	4.497	1.111	0.00879	0.283135±9	+12.8	36.9	15.4
BHVO-2	–	–	0.2764	164.7	16.76	4.472	1.096	0.00877	0.283137±9	+12.9	36.8	15.3
BHVO-1	–	–	0.2786	166.6	16.77	4.492	1.109	0.00880	0.283129±8	+12.6	37.1	15.1
BHVO-2	–	–	0.2773	165.1	16.88	4.475	1.098	0.00879	0.283138±8	+12.9	36.9	15.4

HFSE concentrations of samples marked with an asterisk are from [19]. MgO contents are from: Rurutu: [29], Tubuai: [56], Azores: [33,75], Pitcairn: [74], Samoa: [76]. ε_{Hf} values were calculated relative to a CHUR value of 0.282772 for $^{176}Hf/^{177}Hf$ [24].

Zindler and Hart [28], i.e. HIMU and both enriched mantle varieties (EM-1 and EM-2). HIMU-type samples are from Rurutu and Tubuai Island of the Cook–Austral chain. The Rurutu samples cover lavas from both major volcanic eruption periods (13–10.8 Ma and 1.8–1.1 Ma; [29]). The younger series lavas from Rurutu are more alkaline and have different trace element ratios (e.g., higher La/Yb, Rb/Ba and Ce/Pb ratios, but lower Hf/Sm ratios; [29]) and less radiogenic Pb but more radiogenic Sr isotope ratios compared to the older series lavas. The Tubuai samples are from the 12–5.7 Ma old Herani volcano (except 110B which was collected from the west side of the island). Lavas from the 0.95–0.62 Ma Tedside and Pulawana volcanic suites (Pit89-samples in Table 1) of Pitcairn Island are representative of the EM-1 type OIB. Lavas from Maupiti and Raiatea Island of the Society Island chain (the 4.51–4.35 Ma old Maupiti Island is the oldest subaerial volcanic edifice in the Society chain) and from Savai'i and Upolu Island of western Samoa (0–10 ka old shield and post-shield lavas) are representative of EM-2 type OIB. Samples from the Sete Cidades, Furnas, Nordeste and Fogo volcanoes on Sao Miguel of the Azores islands were also investigated and have isotopic compositions between HIMU and EM-2.

In general, all investigated samples are alkali basalts with MgO contents >4 wt.% (exceptions are the two nephelinites from Rurutu and Tubuai, and two samples from Pitcairn; see Table 1) and have therefore experienced relatively small, but variable amounts of olivine and clinopyroxene fractionation.

3. Results

Zirconium, Hf, Nb, Ta and Lu concentrations as well as Hf isotope compositions are given in Table 1 and have been determined following the procedures described in [30,31] (see Appendix for a detailed description of the analytical methods). All Zr/Hf ratios are superchondritic and range from 35.5 to 45.5 (chondritic ratio: 34.3±0.3; [19]; Fig. 1). In contrast, all Nb/Ta ratios are subchondritic with values between 14.6–17.6 (chondritic ratio: 19.9±0.6; [19]; Fig. 1). HIMU-samples display the largest spread in Zr/Hf (35.5–45.5), with systematic differences in Zr/Hf between the old and young Rurutu samples. The older, less alkaline samples have lower values (35.5–41.0) than the younger, highly alkaline (hawaiitic) samples (42.7–45.1) (see also [29]). Compared to HIMU samples, Zr/Hf ratios in EM-type OIBs are somewhat lower and Zr/Hf ratios in EM-2 samples (Samoa, Society) tend to be lower than in EM-1 (Pitcairn) and Azores samples (Fig. 1b). Nb/Ta ratios in all OIB types are relatively uniform (Nb/Ta=14.6–17.6; Fig. 1b), but small differences exist between different OIB locations with a slightly higher average Nb/Ta ratio in HIMU islands (16.3) than in EM2 (15.4) and EM1 (15.6; Azores: 15.8; Fig. 1). The variation of the Nb/Ta and Zr/Hf ratios are independent of the relative HFSE enrichment or depletion expressed by Nb/La and Zr/Sm ratios, for example. An exception are samples from Samoa, where Nb/Ta displays a slightly negative correlation with Zr/Sm. Taken all OIBs together, Nb/Ta ratios increase moderately with Nb concentrations (Fig. 2a), but samples from each individual island form trends with slightly different slopes (Fig. 2b). Zr/Nb ratios in all OIBs are lower than in average MORB, primitive mantle (PRIMA) and average continental crust (Fig. 2c).

Overall, Zr/Hf ratios are positively correlated with Zr concentrations (Fig. 3), but do not show any systematic variation with $^{176}Hf/^{177}Hf$ ratios except for the Azores samples. HIMU samples have a nearly uniform $^{176}Hf/^{177}Hf$ indicating a homogeneous source with respect to their time integrated Lu/Hf ratio (Fig. 4). The young Rurutu samples are clearly offset from the other HIMU samples and display slightly higher $^{176}Hf/^{177}Hf$ and Zr/Hf indicating a source with a slightly higher time integrated Lu/Hf ratio.

4. Discussion

4.1. HFSE variations related to fractional crystallisation

Mineral–melt partitioning data for mafic systems show that Zr and Hf are nearly an order of magnitude less incompatible than Nb and Ta (see Supplementary data), so that Nb and Ta can be fractionated from Zr and Hf during fractional crystallisation. Extremely low partition coefficients for HFSE between olivine and silicate melt preclude significant changes in Zr/Hf or Nb/Ta ratios by olivine fractionation. It has been shown for natural samples that Zr/Hf ratios in mafic melts are modified by clinopyroxene crystallisation [32,33], which is in agreement with available partition coefficients and with the negative correlations between Zr/Hf ratios and MgO in Tubuai, Pitcairn and Azores samples (Fig. 5). Given the considerable range of Zr/Hf ratios with respect to variations in MgO in all but the Pitcairn and Azores samples (e.g., Zr/Hf=37.5–45.5 ppm in Tubuai samples), it is unlikely, however, that clinopyroxene crystallisation alone can account for the entire range in Zr/Hf (as well as Nb/Ta) in most OIBs. For example, Rayleigh fractionation of 30% clinopyroxene (partition coefficients see Supplementary data) shifts the initial Zr/Hf ratio by about 6–7% (e.g. from 38.0 to 40.7) and the initial Nb/Ta ratio by less than 1% (e.g., from 15.6 to 15.7; Fig. 1), which also explains why there is no correlation between Nb/Ta ratios and MgO contents. As indicated by the crystallisation trajectories in Figs. 2b, c and 3, clinopyroxene, or combined clinopyroxene–olivine fractionation can also not produce the variations in the trace element concentration observed in most sample suites.

Rutile, ilmenite, phlogopite and amphibole are also phases that can fractionate Zr/Hf and Nb/Ta ratios (e.g., [34–39]). The HFSE are compatible in rutile and ilmenite with $D_{Nb/Ta}$ and $D_{Zr/Hf}$ less than 1 (see [40] and references therein). Fractionation of even low amounts of Ti-bearing phases would therefore produce elevated Nb/Ta and Zr/Hf ratios with strongly decreasing Nb and Zr concentrations, a feature that is not observed (see Figs. 2b and 3). Additionally, such phases would affect the Nb/Ta ratios much stronger than the Zr/Hf ratios, the opposite of what is observed in OIBs.

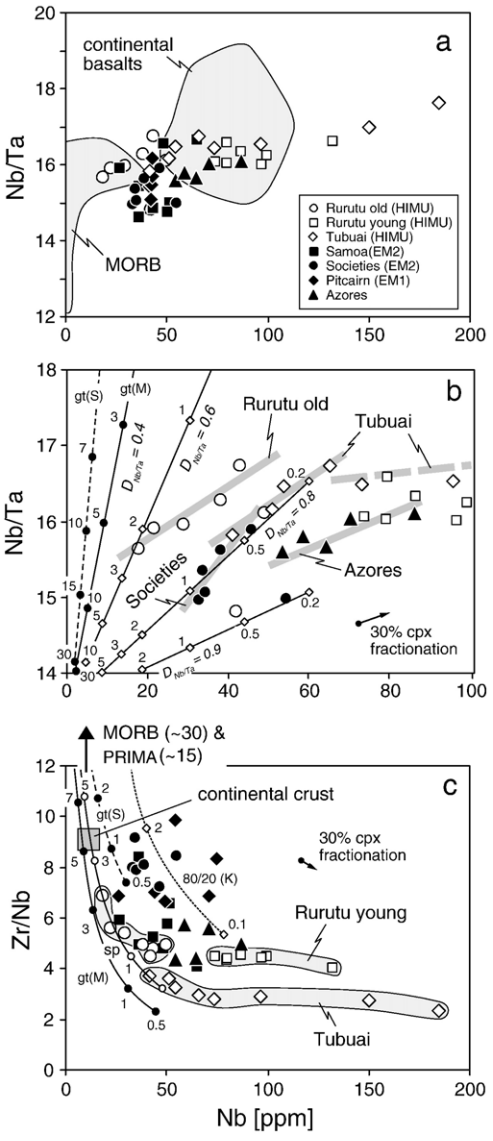

Fig. 2. Nb/Ta and Zr/Nb ratios versus Nb concentration in ocean island basalts. (a) OIBs in comparison to MORB [15] and continental basalts [18]. Nb/Ta ratios are similar to those in MORB, but lower than in most continental basalts. Strong Nb enrichment is observed in some of the HIMU samples. (b) Linear correlations are observed for most individual ocean island suites (thick grey lines, samples from Samoa and Pitcairn are scattered and omitted to improve clarity). Also shown are melting curves for garnet peridotite, calculated by non-modal batch melting for different $^{bulk}D_{Nb/Ta}$ values (black lines, numbers denote degree of melting in percent, gt(M) and gt(S) refer to garnet melting calculated using the partition coefficients of [2,5] and [4], see Appendix for melting parameters). Melting lines for spinel peridotite (not shown) yield similar results due to the similar $^{bulk}D_{Nb/Ta}$ of spinel and garnet peridotite of ~0.4 (details see text and Appendix). The arrow indicates the shift in Nb concentration and Nb/Ta ratios that results from 30% clinopyroxene fractionation. (c) Zr/Nb is low but constant in HIMU samples from Rurutu (young) and Tubuai (grey fields: HIMU samples; continental crust from [73]; MORB and PRIMA from [7]). Melting lines for garnet peridotite as in (b). Also shown is a melting curve for spinel peridotite (white circles; sp) and a melting curve for eclogite with a modal ratio of clinopyroxene/garnet of 80/20, calculated as modal-batch melting and using the partition coefficients of [37] (80/20 (K); see Appendix for melting details).

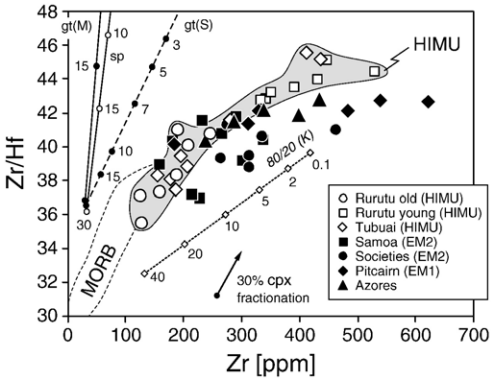

Fig. 3. Zr/Hf versus Zr in ocean island basalts. Also shown is the field for MORB [15]. HIMU and Pitcairn/Azores samples are well correlated, EM2 samples are scattered. Black lines: melting curves for garnet peridotite (gt(M) and gt(S), black circles, see Fig. 2) and spinel peridotite (sp, white circles). Dotted line: melting curve for eclogite as in Fig. 2c. Numbers denote the degree of melting in percent. The arrow indicates the shift in Zr/Hf and Zr concentration produced by 30% Rayleigh fractionation of clinopyroxene, showing that fractionation is not suitable to explain Zr enrichment in most samples.

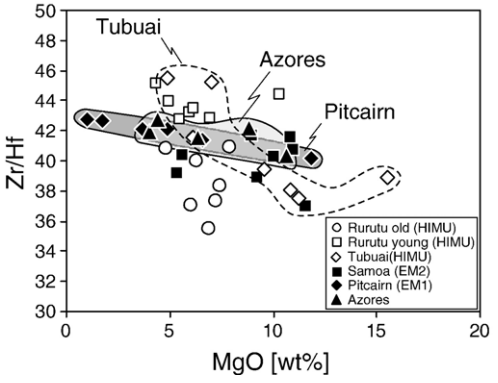

Fig. 5. Zr/Hf ratios versus MgO in ocean island basalts (MgO contents are from: Rurutu: [29], Tubuai: [56], Azores: [33,75], Pitcairn: [74], Samoa: [76]). Slight variations in Zr/Hf ratios over a wide range of MgO in Pitcairn and Azores samples predominantly result from clinopyroxene fractionation.

Phlogopite is not expected to crystallise as primary phase during OIB evolution and would have minor effects on both ratios due to low partition coefficients for all HFSE. The effects of amphibole fractionation on Nb/Ta and Zr/Hf ratios depend on amphibole composition. Low-Mg amphibole, as found in basalts, has $D_{Nb/Ta}>1$ and $D_{Zr/Hf}<1$ [35], and fractionation of such amphibole would lower Nb/Ta ratios in the remaining melt, but increase Zr/Hf ratios, which is not observed (see Fig. 1). In contrast, fractionation of high-Mg amphibole causes similar shifts in Zr/Hf and Nb/Ta ratios as clinopyroxene crystallisation (Fig. 1b).

In conclusion, limited variations of Zr/Hf ratios in OIBs combined with large variations in MgO (e.g., in Pitcairn and Azores samples; Fig. 5) may result from clinopyroxene and/or amphibole crystallisation. Variations in Nb/Ta and Zr/Hf, however, that are expected from crystallisation are small compared to the observed range (Fig. 1b) and thus additional processes such as partial melting, source heterogeneities or mixing and assimilation have to be considered to explain the HFSE composition of OIBs.

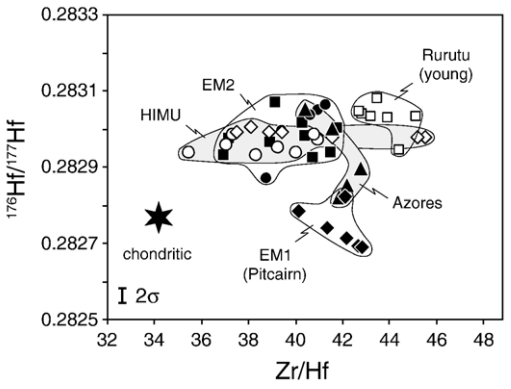

Fig. 4. $^{176}Hf/^{177}Hf$ versus Zr/Hf ratios in ocean island basalts. Nearly invariant $^{176}Hf/^{177}Hf$ in HIMU samples (except the young Rurutu rocks) indicate a source with a homogeneous long-term Lu/Hf ratio. Decreasing $^{176}Hf/^{177}Hf$ in Azores and Pitcairn samples most likely results from recycled sediments in the source of these islands (e.g., [74]).

4.2. HFSE fractionation during partial melting

Nb/Ta ratios in ocean island basalts are decoupled from Zr/Hf ratios, i.e. they do not follow the positive correlation between Zr/Hf and Nb/Ta that is observed for other terrestrial reservoirs (Fig. 1). This is in marked contrast to the expected behaviour of these element pairs and implies either the presence of inherited mantle source heterogeneities or partial melting processes that fractionate Zr/Hf but not Nb/Ta.

In log–log plots [41], only two trace elements with a uniform concentration ratio (and thus identical partition coefficients) yield a linear correlation with a slope of unity. In Fig. 6, log[Ta] versus log[Nb] and log[Hf] versus log[Zr] is shown for all OIBs. The slope for Zr–Hf (0.88 ± 0.03) differs significantly from one, whereas the slope for Nb–Ta (0.95 ± 0.03) is very close to unity. Nb/Ta ratios are therefore less fractionated during partial melting of OIB mantle sources than Zr/Hf ratios and are expected to reflect largely the values of their source.

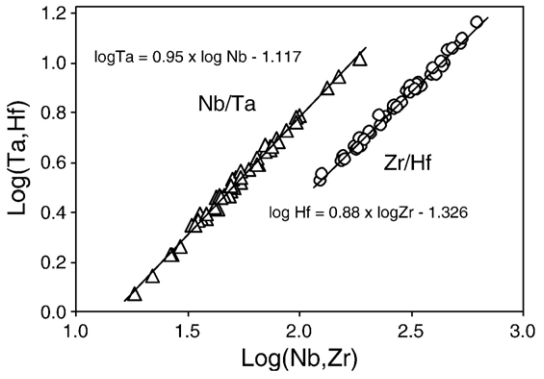

Fig. 6. Plot of log[Ta] versus log[Nb] and log[Hf] versus log[Zr] in ocean island basalts from all locations investigated during this study. The slope of Zr–Hf (0.88±0.03) differs from unity indicating that Zr/Hf ratios may be fractionated during partial melting and fractional crystallisation, in contrast to Nb/Ta ratios where the slope is very close to one (0.95±0.03).

In a plot of Nb/Ta versus Nb concentration, a partial melting trend is expressed by a straight line with a slope proportional to the difference between the two partition coefficients. The linear relationships observed for most individual ocean island suites (Fig. 2b) could thus be interpreted as melting trends. Although fractional crystallisation of clinopyroxene may have caused a slight shift within each suite, having approximately the same direction as partial melting (Fig. 2b), the absolute variations in Nb/Ta resulting from crystallisation are much lower than those observed. Fractionation processes will therefore only lead to a slight underestimation of the degree of melting. Compared to the inferred melting trends in Fig. 2b, calculated melt compositions for garnet and spinel peridotite (non-modal batch melting, see Appendix and Supplementary data) yield melting lines with a steeper slope (Fig. 2b) due to a $^{bulk}D_{Nb/Ta}$ of ~0.4 in spinel and garnet peridotite sources. Experimental partitioning data are thus in contrast to the similar partitioning behaviour of Nb–Ta during OIB source melting as suggested from the log[Ta] versus log[Nb] plot (Fig. 6). On the other hand, the linear relationships in Fig. 2b allow constraining the $^{bulk}D_{Nb/Ta}$ in the source of OIBs by varying the $^{bulk}D_{Nb/Ta}$ within the range expected from experimental data. Arbitrarily lowering the $^{bulk}D_{Ta}$ to obtain $^{bulk}D_{Nb/Ta}$ values between 0.6 and 0.9 underestimates the Nb concentration in OIBs, but the slopes of the melting curves with a $^{bulk}D_{Nb/Ta}$ between 0.8 and 0.9 matches the data trends (Fig. 2b). This implies that either Ta is more incompatible (or Nb is less incompatible) in clinopyroxene and garnet than experimental results indicate, or that a component is present in all OIB sources that increases $D_{Nb/Ta}$ from about 0.4 to 0.9. In contrast to pyrope-rich garnet with $D_{Nb/Ta}<1$, grossular-rich garnet has $D_{Nb/Ta}$ values between about 1.2 and 2.0 [2,37,42]. Grossular-rich garnet is typically found in eclogites (therefore referred to as eclogitic garnet below) but not in peridotite, where garnet is Ca poor [3,42]. Therefore, a $^{bulk}D_{Nb/Ta}$ close to unity suggests the presence of eclogitic garnet and consequently the presence of recycled oceanic crust in the source of OIBs (see also discussions in [43–45]). Rutile, which is a common phase in eclogite, has $D_{Nb/Ta}$ of ~0.6–0.8 (e.g., [46,47]) and may therefore contribute to a higher $D_{Nb/Ta}$ than expected in the source of OIBs. Hence, the slightly different slopes of the melting trends for each ocean island most likely reflect different ratios of eclogite/peridotite involved during melting, or differing amounts of eclogitic garnet present. Samples from Samoa and Pitcairn do not follow a distinct melting trend in Fig. 2b. This suggests that source heterogeneity overwhelms the effects of partial melting, consistent with the large variability of $^{176}Hf/^{177}Hf$ in samples from Samoa and the correlation of $^{176}Hf/^{177}Hf$ with Zr/Hf in the Pitcairn samples (Fig. 4).

As is shown in Fig. 7a, nearly invariant Nb/Ta ratios with respect to Zr/Hf ratios result from melting in the garnet peridotite field, if the partition coefficients of [2,5] are used (black lines in Fig. 7a; see Appendix for a more detailed discussion on partition coefficients and related melt compositions). Virtually no differences in melt composition are observed in this case between melts from spinel (not shown) and garnet facies peridotites as Zr/Hf fractionation is controlled by either clinopyroxene or garnet which have similar $D_{Zr/Hf}$ during mantle melting (~0.5 in clinopyroxene and ~0.6 in pyrope-rich garnet). In contrast, melts calculated for garnet peridotite melting using the partitioning data of [4] display larger variations in Nb/Ta ratios relative to Zr/Hf even for high degrees of partial melting (Fig. 7a). This is caused by lower D-values for Hf and Zr between clinopyroxene and melt in the experiments of [4], which likely reflects a stronger incompatibility of Hf and Zr at higher pressures. According to this, garnet becomes the dominant phase in controlling Zr/Hf fractionation. As $D_{Zr/Hf}$ is about one in the dataset of [4] (see Supplementary data), Zr/Hf fractionation is less pronounced with respect to Nb/Ta fractionation leading to the steeper slope of the melting line in Fig. 7a (see detailed discussion of melt calculations in the Appendix). Nevertheless, both melting models do not fully account for the observed variations in OIBs. Melting curves in Fig. 7a also indicate that unrealistically high degrees of partial melting (>20%) are required to fit the low end of the Zr/Hf range in OIBs, if a primitive mantle composition

with a Zr/Hf ratio of ~34–36 (e.g., [7,19]) and the partitioning data of [2,5] are used. To achieve more realistic degrees of partial melting (<10–15%; [48]), a peridotite source with a lower Zr/Hf ratio (~27) would be required (Fig. 7a). Given that only some portions of the depleted mantle may be low in Zr/Hf [17], whereas most other estimates for Zr/Hf in the depleted and primitive mantle are between 32 and 40 [7,49,50], it is unlikely, that the Zr/Hf ratio in the OIB source is much lower than ~34–36. It is therefore more plausible to call for the presence of eclogitic garnet, as suggested from Nb/Ta versus Nb systematics, which results in a higher $^{bulk}D_{Zr/Hf}$ in the source of OIBs and thus lower Zr/Hf ratios in the melts. Two sets of eclogite melting curves are shown in Fig. 7a and b, representing two different sets of partition coefficients ([37,42]; see Appendix for details). Eclogite melting was modelled as modal batch melting of a clinopyroxene/garnet assemblage with modal ratios of 70/30 and 80/20, which may cover the expected range of bulk compositions in MORB-like eclogites [42]. Although the two datasets yield opposite melting trends with respect to Nb/Ta owing to strongly different $^{bulk}D_{Nb/Ta}$ (>1 and <1, respectively), Nb/Ta fractionation is more pronounced for eclogite melting than for melting of either garnet or spinel peridotite, and Zr/Hf is invariably lower. Addition of eclogite melts to melts from a garnet peridotite source with a chondritic or slightly subchondritic Zr/Hf ratio could thus account for the Nb/Ta and Zr/Hf ratios in OIBs. That is, mixing trajectories

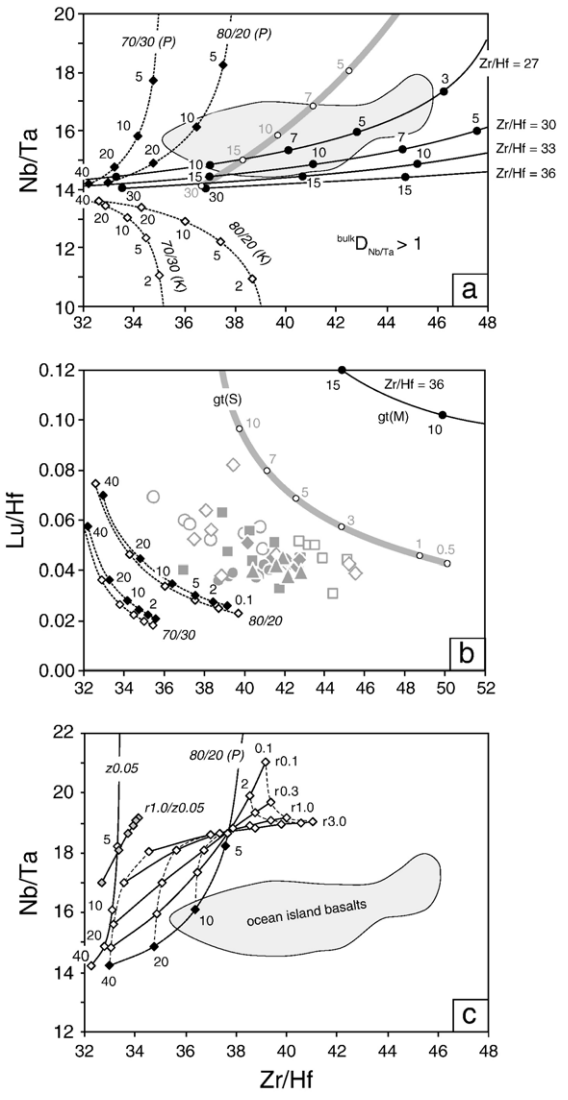

Fig. 7. Melting curves for garnet peridotite and eclogite in terms of Nb/Ta and Lu/Hf versus Zr/Hf ratios, calculated for various compositions and using different sets of partition coefficients. (a) Melting curves for garnet peridotite using the partitioning data of [2,5] were calculated for Zr/Hf ratios between 27 and 36 in the source (solid black lines) and indicate, that only a source with low Zr/Hf is suitable to shift the melting trajectory into the datafield. If garnet peridotite melting is calculated using the partition coefficients of [4] (thick grey line, Zr/Hf in the source=36; see Appendix), Nb/Ta variations are higher even for high degrees of partial melting. Also shown are melting curves for eclogites with different ratios of modal clinopyroxene/garnet (modal batch melting), using two different sets of partition coefficients: Melting curves indicated by black diamonds were calculated using the partitioning data of [42]. Melting curves indicated by white diamonds were calculated using the partition coefficients of [37]. Although both sets of partition coefficients yield similar results with respect to Zr/Hf ratios, the Nb/Ta ratios in eclogite melts are strongly different due to strongly different $^{bulk}D_{Nb/Ta}$ (<1 in [42] and >1 in [37], respectively). Numbers on tick marks denote the degree of melting in percent, numbers in italics denote the modal ratio of clinopyroxene/garnet in eclogite. See text and Appendix for details. (b) Independent of the partitioning dataset used, melting of garnet peridotite (gt(M) and gt(S), calculated using the partition coefficients of [2,5] and [4], respectively) fails to account for the low Lu/Hf ratios in OIBs, which in turn are well explained assuming a mixing process between melts from eclogite and garnet peridotite (eclogite melting curves calculated as in (a), note that both sets of partition coefficients yield very similar results). Melting of spinel peridotite will produce higher Lu/Hf ratios at a given Zr/Hf than melting of garnet peridotite and is thus not considered. (c) Model melting curve of a rutile-free eclogite (black diamonds, 80/20 clinopyroxene/garnet, partition coefficients from [42]) compared to calculated melt compositions from rutile and zircon bearing eclogites (white diamonds, 80/20 clinopyroxene/garnet+rutile/zircon, batch melting, rutile partition coefficients from [46], partition coefficients for Zr and Hf for zircon are assumed to be equal and >1000 to account for the fact that these elements are major phases in zircon and thus are "fully compatible"; e.g., [54]). r0.1, r0.3, r1.0, r3.0 indicate 0.1%, 0.3%, 1.0% and 3.0% rutile present, z0.05 indicates the presence of 0.05% zircon. Numbers denote the degree of melting in percent. The variation of Nb/Ta ratios in eclogite melts is strongly reduced by the presence of rutile and even low amounts of zircon drop the Zr/Hf ratios in the melt dramatically. The presence of both, rutile and zircon strongly reduces the range of Zr/Hf and Nb/Ta ratios in the melts (for details see text and Appendix).

between eclogite melts that were produced by melting degrees >5% and melts from garnet peridotite sources intersect the OIB datafield (Fig. 7a), independent of whether the partition coefficients of [37] or [42] are used to calculate eclogite melting. In the experiments of van Westrenen et al. [2] (run 12, Py65, 3 GPa) and Hauri et al. [51] Zr and Hf are compatible in eclogitic garnet with $D_{Zr/Hf}>1$ (see Supplementary data). Using these partition coefficients to calculate eclogite melts (not shown) will result in similar melting curves compared to those in the upper part of Fig. 7a, but at modal abundances for garnet of only a few percent. For higher modal amounts of garnet, e.g. in the range typically found in eclogites (20–30%; e.g. [42]), the $D_{Zr/Hf}$ in the bulk assemblage becomes dominated by the garnet, and Zr/Hf ratios in the melt are lower than in the source. Note that despite the different Zr–Hf fractionation, this scenario is consistent with the proposed mixing model between eclogitic and garnet peridotite melts. The presence of eclogite in the source of most or even all OIBs is also strongly supported by Lu/Hf ratios. These are consistently lower in all OIBs than in melts produced from pure spinel or garnet peridotite sources, but are higher than in eclogite derived melts (Fig. 7b). Mixing of garnet peridotite and eclogite melts is thus also in agreement with the combined Lu/Hf–Zr/Hf data, which further suggest eclogites in the OIB sources that have a modal abundance of garnet >20%, eclogite melting degrees up to 20% and low degree melting of ambient garnet peridotite (<10%). These estimates are in good agreement with the lower solidus temperature of eclogite compared to peridotite (e.g., [42]).

Rutile is a common phase in eclogites (e.g., [20,52]) and its role has to be considered in any eclogite melting model, as it hosts a significant portion of the HFSE, particularly Nb and Ta (e.g., [20]). The same is valid for zircon with respect to Zr and Hf [53,54], although zircon may not generally be found in eclogites (e.g., [52,55]). Calculated Nb/Ta and Zr/Hf ratios in melts from rutile and zircon bearing eclogites are shown in Fig. 7c. Due to a $D_{Nb/Ta}$ of ~0.7 and D_{Nb} ~100 in rutile (e.g., [46]), the presence of rutile in eclogite melt residues reduces the variability of Nb/Ta ratios in the melt dramatically without significantly affecting Zr/Hf ratios. Thus the lack of correlation between Nb/Ta and Zr/Hf ratios supports the presence of rutile bearing eclogites in the source of OIBs. Residual rutile will produce melts with high Zr/Nb ratios (not shown), whereas residual zircon will have the opposite effect. The low Zr/Nb ratios observed in most OIBs therefore even suggest the presence of zircon in the eclogite melting assemblage. Its amount, however, has to be exceedingly low (<0.05%) due to the high compatibility of Zr and Hf in zircon that otherwise would result in extremely low Zr and Hf concentrations and very high Lu/Hf ratios in the melts. In addition, zircon does not significantly fractionate Zr/Hf ratios [54] and thus elevated amounts in the melting assemblage would result in melts having invariant and low (i.e. source like) Zr/Hf ratios.

4.3. Constraints on a superchondritic Nb/Ta reservoir in the mantle?

Assuming a chondritic Nb/Ta ratio for the bulk Earth, the overall subchondritic Nb/Ta ratios in terrestrial silicate reservoirs indicate an apparent Nb deficit in the accessible silicate portion of the Earth (Fig. 1). Several authors thus postulated the presence of a so far unsampled reservoir with a complementary, superchondritic Nb/Ta ratio, which is thought to be subducted eclogitic slabs in the deep mantle with Nb/Ta ratios between 24 and 33 [20,21]. Such a hidden mantle reservoir was also suggested to account for the mass imbalance in the terrestrial Hf–Nd isotope inventory and for the ^{142}Nd-excess in terrestrial rocks [24–26]. By definition, there cannot be any direct evidence either in favour of or against the existence of such a hidden mantle reservoir. However, assuming that HIMU OIBs from Tubuai, for example, contain 20–30% of recycled oceanic crust [56] with an eclogitic Nb/Ta of ~30 [20], the Nb/Ta ratio in HIMU basalts should be at least 25% higher compared to MORB and other OIBs. This is not observed, which indicates that the recycled eclogitic component in the source of HIMU lavas most likely has a low Nb/Ta ratio. This is in agreement with Nb/Ta ratios observed in MORB-derived eclogites (Nb/Ta=13.2±1.5; 1σ, n=28; [57]), and with high-precision HFSE data of island arc rocks where Nb/Ta ratios vary between 11.3 and 17.4 and are indistinguishable from MORB [40]. Such a similarity between the Nb/Ta of pristine MORB, their eclogite facies equivalents, and island arc rocks implies that the present-day metamorphic processes in subduction zones do not lead to a significant fractionation of Nb/Ta.

Based on the observation that in Hf–Nd isotope space the mantle array (i.e. oceanic basalts) does not intersect the composition of the bulk silicate Earth (BSE), an isolated mantle reservoir was also postulated to balance the global Hf–Nd isotope inventory [24]. Although this conclusion was recently alleviated by a revised and slightly higher chondritic ^{176}Hf/^{177}Hf value [58], the postulated hidden reservoir is thought to be characterised by low ε_{Hf} for given ε_{Nd}, i.e. samples that tap this reservoir are required to plot below the mantle

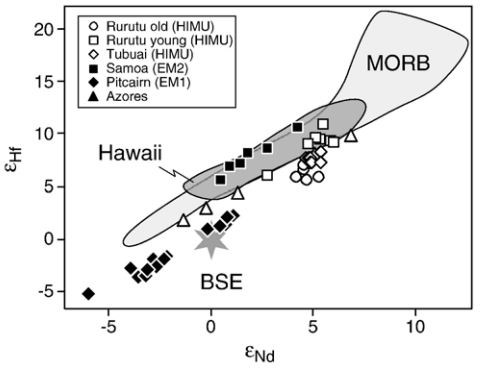

Fig. 8. ε_{Hf} versus ε_{Nd} in ocean island basalts. HIMU and Pitcairn (EM 1) samples are most offset from the mantle array with lower ε_{Hf} for given ε_{Nd}. Data sources: Hawaii: [77]; MORB: [78]; Pitcairn: this study and [74]. ε_{Nd} from Rurutu and Tubuai are from [29,56], ε_{Nd} of Samoa from [76] and Azores from [75]. BSE = bulk silicate Earth.

array. This is observed in HIMU samples from Rurutu and Tubuai (Fig. 8). There is, however, no increase of Nb/Ta with the deviation of ε_{Hf} from the terrestrial Hf–Nd isotope array in HIMU lavas (Table 1), suggesting that a potential reservoir of subducted oceanic crust in the Earth's mantle most likely has a subchondritic Nb/Ta.

In previous studies, the size of the hidden eclogitic reservoir was estimated to be about 1–9% of the mass of the BSE [20,21]. It was further suggested that this reservoir was generated during the Hadean by intense slab melting driven by high mantle temperatures. A Hadean age is consistent with the subchondritic Nb/Ta ratios in early Archean greenstones [19] that overlap with the Nb/Ta composition of present day MORB (~15) and indicate that the Nb depletion in the silicate Earth must have occurred early. It seems unlikely, however, that a complementary Nb enriched reservoir could be isolated in the Earth's lower mantle for a long period of time without being disseminated by mantle convection, and thus without being sampled by any terrestrial magmatism. Moreover, taking the revised chondritic Nb/Ta ratio of 19.9 [19] instead of the value used earlier (17.4; [59]), the Nb-deficit of the accessible silicate Earth and hence the volume of the postulated hidden mantle reservoir increases to more than 10% of the mass of the BSE, making its isolation over at least 3.5 Ga even more difficult.

In a recent study, Münker et al. [19] observed that not only the Earth, but also the Moon is depleted in Nb, i.e. the lunar sample array also displays an offset from the chondritic ratios in terms of Nb/Ta versus Zr/Hf (Fig. 1a). In contrast, no selective Nb depletion is resolvable for Martian samples and asteroids (eucrites and angrites). Together with experimental data [27], this was taken as evidence that Nb might be slightly more siderophile than Ta at higher pressures, i.e. during core formation, leading to superchondritic Nb/Ta in the Earth's core. As core formation occurred very early in Earth's history (~4.533 Ga; [60]), the Nb depletion of the silicate Earth must have occurred earlier than formation of the earliest crust. Niobium storage in the core was also suggested by [61], who observed superchondritic Nb/Ta ratios in some OIBs and suggested that these high ratios are due to Nb addition from the core. However, there is little support for a direct core contribution to mantle melts from the high-precision Nb/Ta data presented here. Assuming that the core contains about 0.47 ppm Nb [19] and plume-type mantle contains about 0.2–0.8 ppm Nb (e.g., [62]) and Nb/Ta=15.9 (this study), addition of more than 3–4% core material (Nb/Ta >85, see Appendix) shifts the Nb/Ta outside the array defined by the OIB data. It is therefore concluded that, in agreement with inferences from W isotope data [63], only small amounts of core material are sampled by oceanic volcanism.

4.4. Evolution of Zr/Hf and Nb/Ta in mantle and crust

In contrast to the first order silicate fractionation trend defined by increasing Nb/Ta with increasing Zr/Hf in terrestrial reservoirs (Fig. 1a), Nb/Ta ratios in ocean island basalts are nearly constant at variable Zr/Hf ratios (Fig. 1b). Hence, Nb/Ta is constant in major portions of the enriched mantle (15.9±0.6) and similar to some portions of the upper depleted mantle as suggested by high-precision data of representative MORB samples ([15,19]; Fig. 1). Nb/Ta therefore appears to be distinctly higher (~15–16) in most portions of the mantle than in the continental crust (Nb/Ta=12–13; [14]) and in the BSE (Nb/Ta=14.0±0.3; [19]; Fig. 1a). Hence, most parts of the accessible mantle and the continental crust appear to be complementary reservoirs with respect to BSE. Crust–mantle differentiation is thus most likely the process responsible for Nb/Ta fractionation within the silicate Earth and resulting in a slight Nb *enrichment* of the Earth's whole mantle and depletion of the newly formed crust relative to BSE. This fractionation event must have taken place after core formation, during which the overall subchondritic Nb/Ta ratio of the BSE was established [19]. Archean greenstones have Nb/Ta ratios virtually identical to Nb/Ta ratios in modern OIBs and enriched MORB ([19]; Fig. 1a). Early Archean magmatism consequently tapped a mantle source with Nb/Ta of 15–16 suggesting that Nb/Ta fractionation between major Earth reservoirs

(mantle and continental crust) occurred early in Earth's history. An early differentiation process of the silicate Earth (prior to 3.8 Ga) was also suggested from Hf–Nd isotope systematics of early Archean rocks [64] and from $^{142}Nd/^{144}Nd$ data from terrestrial rocks and chondrites [26,65].

The lower Nb/Ta in the continental crust relative to BSE requires a petrogenetic process that selectively depletes Nb relative to Ta during crust formation. In mantle peridotite and rutile bearing eclogites, such as modern subducting slabs, Nb is slightly more incompatible than Ta during melting [34,46,47], resulting in slightly elevated Nb/Ta ratios in primitive mantle melts and island arc rocks [10,40]. Low Nb/Ta, however, can be explained by melting of garnet amphibolites in subduction zones as suggested by [39]. $D_{Nb/Ta}$ between low-Mg amphibole and melt is >1 such that Nb is preferentially retained by amphibole bearing residues, resulting in melts with lower Nb/Ta ratios. Since the subducted garnet–amphibolite residues will have elevated Nb/Ta (>14) after slab melt extraction, such a process also provides a likely explanation for the elevated Nb/Ta ratios in OIBs and many MORBs relative to BSE. Following this model, major portions of the continental crust must have been formed by melting of subducted slabs in the garnet amphibolite stability field.

5. Conclusions

New high-precision HFSE concentration data of ocean island basalts show that despite their similar geochemical characteristics, Nb/Ta and Zr/Hf ratios are variable and deviate significantly from the chondritic values. Variations in Zr/Hf on the order of 5–15% that correlate with variations in MgO are controlled by fractionation of clinopyroxene and/or Mg-rich amphibole, whereas the larger variations generally observed suggest an additional influence of partial melting of a spinel or garnet facies mantle peridotite. Variations in Nb/Ta that are caused by fractional crystallisation of clinopyroxene are less than 1% and thus negligible. In order to account for the observed range in Zr/Hf and Nb/Ta ratios, the presence of grossular-rich garnet in the mantle source of OIBs is required, which in turn implies the presence of recycled eclogite or garnet pyroxenite.

The overall subchondritic Nb/Ta ratios in mantle derived rocks and the continental crust are consistent with the proposed Nb depletion of the silicate portion of the Earth during core formation [19] and argue against the presence of a complementary superchondritic Nb/Ta reservoir (>20) in the Earth's mantle. Nb/Ta ratios in OIBs are virtually identical to values in many MORB, and higher than the estimated Nb/Ta ratio in the continental crust (~12–13) and the bulk-silicate Earth (~14). This indicates a slight Nb *enrichment* of major portions of the mantle relative to the bulk-silicate Earth that likely is the consequence of subduction related crust–mantle differentiation. This differentiation process must have occurred early in the Earth's history, in agreement with evidence from Hf- and ^{142}Nd-isotope systematics [66,67], as Archean greenstones have Nb/Ta ratios very similar to those in recent OIB and many MORB and thus tapped a geochemically similar mantle source. Melting of subducted eclogitic crust fails to produce low Nb/Ta ratios in island-arc rocks [40], i.e. the precursors of the continental crust. Early crust–mantle differentiation involving partial melting of amphibolitic slabs, however, provides sufficiently low Nb/Ta in coexisting melts and is therefore thought to play a significant role for Nb/Ta fractionation between the Earth's mantle and crust.

Acknowledgements

We thank numerous scientists for kindly providing samples, namely Catherine Chauvel, Marcel Regelous, Colin Devey and Karsten Haase. Marcel Regelous is thanked for providing unpublished data and K.P. Jochum for supplying the standards BHVO-1 and BHVO-2. Discussions with A.W. Hofmann and S. Jung during an early stage of the present study are acknowledged. Comments by Robbie King and an anonymous reviewer are greatly appreciated. They helped to improve the manuscript significantly and made us consider the role of rutile and zircon during eclogite melting. Many thanks to Rick Carlson for editorial handling. This work was supported by the Deutsche Forschungsgemeinschaft (DFG grant Me 1717/1-2, 4-1). AS acknowledges support from the DFG by grant STR 853/2-1.

Appendix A. Analytical techniques

Sample powders (50–100 mg) prepared in agate were spiked with a mixed ^{180}Ta–^{180}Hf–^{176}Lu–^{94}Zr tracer and dissolved in concentrated HF–HNO_3 (~4:1) at about 120 °C for >48 h in Savilex© beakers. After drying down three times with concentrated HNO_3 containing trace HF (<0.05 M), and complete dissolution in 6 M HCl (containing trace HF), the dried down residues were redissolved in 3 M HCl prior to column separation. Individual HFSE cuts and Lu were purified using Ln-Spec© and anion-exchange resins. Zirconium, Hf, Ta and Lu concentrations were obtained by isotope-dilution using a Micromass Isoprobe multiple-collector

ICPMS at Münster. Hafnium isotope ratio measurements were normalised to $^{179}Hf/^{177}Hf = 0.7325$ and $^{176}Hf/^{177}Hf$ data are given relative to a JMC 475 value of 0.282160 (see [31]). Repeated measurements of the Ames metal Hf standard (isotopically indistinguishable from JMC 475) resulted in 0.282160 ± 0.000018 (2σ external, $n = 86$) for measuring concentrations between 24 and 80 ppb. The concentrations of Nb were determined from measured $^{93}Nb/^{90}Zr$ ratios against a Zr–Nb standard that was gravimetrically prepared from 99.9% pure Ames metals. The external reproducibility is better than ±1% for Lu, Ta, Zr and Hf concentrations, and better than ±4% for Nb concentrations. External reproducibility for Lu/Hf, Nb/Ta and Zr/Hf ratios is better than ±1%, ±4% and ±0.6% (2σ), respectively. Results of repeated analyses of reference materials BHVO-1 and BHVO-2 are given in Table 1.

Appendix B. Modelling parameters

B.1. Partition coefficients

Partitioning data for modelling mantle melting and crystal fractionation often lack values for Ta or are restricted to the partitioning behaviour of clinopyroxene (e.g., [1,68–70]). Here we used the experimental partitioning datasets of [2,4,5,42,71] for calculating fractional crystallisation and mantle melting in spinel and garnet bearing systems (see Supplementary data). The study of [5] considers all HFSE as well as major mantle phases and partition coefficients were determined at 1.5 GPa and 1315 °C close to the anhydrous solidus of refractory lherzolite. Using these values minimises the necessity to combine values for different elements from different experiments. Values for garnet from [2] are those for pyrope-rich garnet (run 11, Py84), where Zr, Hf and Nb partition coefficients are within or close to the range determined by others (e.g., [4,69,70]). Although absolute values for partition coefficients are a function of pressure, temperature, composition and degree of melting, the relative partitioning behaviour of the HFSE is less sensitive to these parameters as is demonstrated by fairly constant $^{cpx/melt}D_{Zr/Hf}$ and $^{cpx/melt}D_{Nb/Ta}$ for various experiments (see Supplementary data). $^{cpx/melt}D_{Zr/Hf}$ is consistently close to 0.5, so that clinopyroxene will dominate Zr/Hf fractionation in garnet free systems. Values for $^{cpx/melt}D_{Nb/Ta}$ in refractory and fertile lherzolite are also very similar (0.34 versus 0.38; [1,5]), indicating that changing phase proportions and compositions will have negligible effects on the relative partitioning behaviour of Nb and Ta. The partitioning behaviour of the HFSE between garnet and melt depends on garnet composition [2,37,42]. For pyrope-rich garnet, all HFSE are incompatible with $D_{Zr/Hf} < 1$ in most cases, whereas for higher Ca contents, i.e. in eclogitic garnet, Zr and Hf become less incompatible and $D_{Zr/Hf}$ becomes >1 [2,3,37,42,51]. Niobium and Ta are incompatible in garnet, with $D_{Nb/Ta}$ around unity for various compositions [2]. In spinel, HFSE are incompatible with $D_{Nb/Ta} = 1.2$ and $D_{Zr/Hf} = 1.3$. The partition coefficients of [4] have frequently been used to model mantle melting in the garnet stability field, but do not include values for Ta. Therefore, where these values are used during this study, they are from run RD 1097-5 and -7 where clinopyroxene coexists with orthopyroxene and garnet at 3.2 and 3.4 GPa and the missing values for Ta were approximated by using the $D_{Nb/Ta}$ ratios of [5] for orthopyroxene and clinopyroxene, and the $D_{Nb/Ta}$ ratio of [2] for garnet.

In eclogite–melt systems, two different sets of partition coefficients ([42] and [37]) are used to evaluate the differences in melt compositions that result from uncertainties in the partitioning data. $D_{Zr/Hf}$ is complementary between garnet/melt (>1) and clinopyroxene/melt (<1) in eclogite systems [2,3,37,42,51], such that Zr/Hf fractionation during eclogite melting is controlled by modal abundances of the melting assemblage. In general, given that eclogite may typically contain about 20–30% modal garnet (e.g. [42] and references therein), melting of eclogite will produce melts with lower Zr/Hf ratios than melting of mantle garnet peridotite and Zr/Hf fractionation during eclogite melting will be less pronounced than during melting of garnet peridotite sources. $D_{Nb/Ta}$ between eclogitic garnet and melt is between 0.76 and 2.0. Strongly different values for $D_{Nb/Ta}$ between clinopyroxene and melt in eclogite systems result from the datasets of [37] ($D_{Nb/Ta} = 1.75$) and [42] ($D_{Nb/Ta} = 0.31$–0.45), which has significant consequences on calculated Nb/Ta ratios in eclogite melts. Using the partitioning data of [42], Nb/Ta variations will be low for similar modal abundances of garnet and clinopyroxene as will be Zr/Hf ratios. In eclogites, where clinopyroxene typically dominates the modal composition, Nb/Ta ratios in the melt are higher than in the source. In contrast, using the values of [37], Nb/Ta will be fractionated independently of modal abundances of garnet and clinopyroxene and melts will have low Nb/Ta ratios. Except for Nb/Ta, however, the partitioning data for clinopyroxene and garnet of [37] and [42] result in similar D-ratios and therefore produce nearly identical melt compositions with respect to Zr/Hf and Lu/Hf. Partition coefficients for rutile used to calculate melt compositions from rutile bearing eclogites are those of [46] that lie well within the range of other published values (e.g., [47]).

B.2. Melting calculations

Melting spinel and garnet peridotite was modelled as non-modal batch melting, which yields very similar results than fractional and accumulated fractional melting. Source modes and melting reactions were taken from [72] and are for the garnet stability field: source mode: 0.53 ol : 0.04 opx : 0.38 cpx : 0.05 gt, melt mode: 0.05 ol : −0.49 opx : 1.31 cpx : 0.13 gt, and for the spinel stability field: source mode: 0.53 ol : 0.15 opx : 0.3 cpx : 0.02 sp, melt mode: 0.375 ol : −0.5 opx : 1.125 cpx. To evaluate the effect on HFSE concentrations and ratios by using different modal abundances, we also tested the modes of [69]. The variations are found to be only subordinate with respect to variations in partition coefficients. Hence, different modal compositions have not further considered. Initial trace element abundances used in modelling are primitive mantle values taken from [7], except for Nb, for which the concentration in the source was reduced from 0.618 ppm to 0.491 ppm to fit the requirement of a Nb/Ta of 14.0 in the bulk-silicate Earth after core formation [19].

Eclogite melting was calculated as modal batch melting of clinopyroxene/garnet assemblages. Starting compositions are averaged eclogite concentrations from [57] (excluding group III samples which display an enriched OIB-like trace element pattern). These values may be a good estimate for average subducted oceanic lithosphere, in which the concentrations of the immobile HFSE have to be markedly lower than in MORB. This is due to the presence of depleted gabbros and ultramafic cumulates in the subducting assemblage, which cause a "dilution effect" and thus reduce the concentrations of immobile incompatible trace elements.

B.3. Core addition calculations

Core contribution to the OIB mantle source was calculated assuming that chondrites contain 0.437 ppm Nb (average chondritic value calculated from analyses given in [19]), Nb/Ta = 19.9, and that Nb/Ta in the bulk-silicate Earth after core segregation was 14.0 [19]. Given the mass fraction of the core (0.33) and its estimated Nb concentration (0.47 ppm; [19]), mass balance considerations between the core, BSE and chondrites suggest a maximum Ta concentration in the core of 0.006 ppm, yielding a minimum Nb/Ta ratio of ~85 (which is close to the value of ~75 given by [22]). Note that the calculated Ta concentration of the core and hence its Nb/Ta ratio is very sensitive to the estimated Nb concentration in chondrites in that a slightly higher chondritic Nb concentration results in a much higher Nb/Ta ratio in the core.

Appendix C. Supplementary data

Supplementary data associated with this article can be found, in the online version, at doi:10.1016/j.epsl.2006.11.027.

References

[1] J.D. Blundy, J.A.C. Robinson, B.J. Wood, Heavy REE are compatible in clinopyroxene on the spinel lherzolite solidus, Earth Planet. Sci. Lett. 160 (1998) 493–504.
[2] W. van Westrenen, J. Blundy, B. Wood, Crystal-chemical controls on trace element partitioning between garnet and anhydrous silicate melt, Am. Mineral. 84 (1999) 838–847.
[3] W. van Westrenen, J.D. Blundy, B.J. Wood, High field strength element/rare earth element fractionation during partial melting in the presence of garnet: implications for identification of mantle heterogeneities, Geochem. Geophys. Geosyst. 2 (2001) (paper number 2000GC000133).
[4] V.J.M. Salters, J.E. Longhi, M. Bizimis, Near mantle solidus trace element partitioning at pressures up to 3.4 GPa, Geochem. Geophys. Geosyst. 3 (2002) (Paper number 2001GC000148).
[5] P. McDade, J.D. Blundy, B.J. Wood, Trace element partitioning on the Tinaquillo Lherzolite solidus at 1.5 GPa, Phys. Earth Planet. Inter. 139 (2003) 129–147.
[6] W.M. White, A.W. Hofmann, Sr and Nd isotope geochemistry of oceanic basalts and mantle evolution, Nature 296 (1986) 821–825.
[7] A.W. Hofmann, Chemical differentiation of the Earth: the relationship between mantle, continental crust, and oceanic crust, Earth Planet. Sci. Lett. 90 (1988) 297–314.
[8] A.W. Hofmann, Mantle geochemistry: the message from oceanic volcanism, Nature 385 (1997) 219–229.
[9] T. Plank, W.M. White, Nb and Ta in arc and mid-ocean basalts, EOS 76 (1995) 655.
[10] A.J. Stolz, K.P. Jochum, B. Spettel, A.W. Hofmann, Fluid-and melt-related enrichment in the subarc mantle: evidence from Nb/Ta variations in island arc basalts, Geology 24 (1996) 587–590.
[11] K.P. Jochum, J. Pfänder, J.E. Snow, A.W. Hofmann, Nb/Ta in mantle and crust, EOS 78 (1997) 804.
[12] Y. Niu, R. Batiza, Trace element evicence from seamounts for recycled oceanic crust in the eastern Pacific mantle, Earth Planet. Sci. Lett. 148 (1997) 471–483.
[13] C. Münker, Nb/Ta fractionation in a Cambrian arc/back-arc system, New Zealand: source constraints and application of refined ICPMS techniques, Chem. Geol. 144 (1998) 23–45.
[14] M.G. Barth, W.F. McDonough, R.L. Rudnick, Tracking the budget of Nb and Ta in the continental crust, Chem. Geol. 165 (2000) 197–213.
[15] A. Büchl, C. Münker, K. Mezger, A.W. Hofmann, High-precision Nb/Ta and Zr/Hf ratios in global MORB, Geochim. Cosmochim. Acta 66 (2002) A108 (Spec. Suppl.).
[16] F. Kalfoun, D. Ionov, C. Merlet, HFSE residence and Nb/Ta ratios in metasomatised, rutile bearing mantle peridotites, Earth Planet. Sci. Lett. 182 (2002) 1–17.
[17] S. Weyer, C. Münker, K. Mezger, Nb/Ta, Zr/Hf and REE in the depleted mantle: implications for the differentiation history of the crust–mantle system, Earth Planet. Sci. Lett. 205 (2003) 309–324.
[18] J.A. Pfänder, C. Münker, K. Mezger, A.W. Hofmann, In search of a superchondritic Nb/Ta reservoir: high-precision Nb/Ta and

Zr/Hf ratios in ocean island and intraplate basalts, Geochim. Cosmochim. Acta 66 (2002) A597 (Spec. Suppl.).
[19] C. Münker, J.A. Pfänder, S. Weyer, A. Büchl, T. Kleine, K. Mezger, Evolution of planetary cores and the Earth–Moon system from Nb/Ta systematics, Science 301 (2003) 84–87.
[20] R.L. Rudnick, M. Barth, I. Horn, W.F. McDonough, Rutile-bearing refractory eclogites: missing link between continents and depleted mantle, Science 287 (2000) 278–281.
[21] B. Kamber, K.D. Collerson, Role of 'hidden' deeply subducted slabs in mantle depletion, Chem. Geol. 166 (2000) 241–254.
[22] K.P. Jochum, A.W. Hofmann, M. Seufert, B. Stoll, Niobium in planetary cores: consequences for the interpretation of terrestrial Nb systematics, Geochim. Cosmochim. Acta 66 (2002) A368 (Spec. Suppl.).
[23] R.P. Rapp, N. Shimizu, M.D. Norman, Growth of early continental crust by partial melting of eclogite, Nature 425 (2003) 605–609.
[24] J. Blichert-Toft, F. Albarède, The Lu–Hf isotope geochemistry of chondrites and the evolution of the mantle–crust system, Earth Planet. Sci. Lett. 148 (1997) 243–258.
[25] M. Bizzarro, A. Simonetti, R.K. Stevenson, J. David, Hf isotope evidence for a hidden mantle reservoir, Geology 30 (2002) 771–774.
[26] M. Boyet, R.W. Carlson, Nd-142 evidence for early (>4.53 Ga) global differentiation of the silicate Earth, Science 309 (2005) 576–581.
[27] J. Wade, B.J. Wood, The Earth's 'missing' niobium may be in the core, Nature 409 (2001) 75–78.
[28] A. Zindler, S. Hart, Chemical geodynamics, Annu. Rev. Earth Planet. Sci. 14 (1986) 493–571.
[29] C. Chauvel, W. McDonough, G. Guille, R. Maury, R. Duncan, Contrasting old and young volcanism in Rurutu Island, Austral chain, Chem. Geol. 139 (1997) 125–143.
[30] S. Weyer, C. Münker, M. Rehkämper, K. Mezger, Determination of ultra low Nb, Ta, Zr, and Hf concentrations and precise Nb/Ta and Zr/Hf ratios by isotope dilution analyses with multiple collector ICP-MS, Chem. Geol. 187 (2002) 295–313.
[31] C. Münker, S. Weyer, E. Scherer, K. Mezger, Separation of high field strength elements (Nb, Ta, Zr, Hf) and Lu from rock samples for MC-ICPMS measurements, Geochem. Geophys. Geosyst. 2 (2001) (Paper number 2001GC000183).
[32] K. David, P. Schiano, C.J. Allègre, Assessment of the Zr/Hf fractionation in oceanic basalts and continental materials during petrogenetic processes, Earth Planet. Sci. Lett. 178 (2000) 285–301.
[33] C. Beier, K.M. Haase, T.H. Hansteen, Magma evolution of the Sete Cidades volcano, Sao Miguel, Azores, J. Petrol. 47 (2006) 1375–1411.
[34] S.F. Foley, M.G. Barth, G.A. Jenner, Rutile/melt partition coefficients for trace elements and an assessment of the influence of rutile on the trace element characteristics of subduction zone magmas, Geochim. Cosmochim. Acta 64 (2000) 933–938.
[35] M. Tiepolo, R. Vannucci, R. Oberti, S. Foley, P. Bottazzi, A. Zanetti, Nb and Ta incorporation and fractionation in titanian pargasite and kaersutite: crystal-chemical constraints and implications for natural systems, Earth Planet. Sci. Lett. 176 (2000) 185–201.
[36] M. Tiepolo, P. Bottazzi, S.F. Foley, R. Oberti, R. Vannucci, A. Zanetti, Fractionation of Nb and Ta from Zr and Hf at mantle depths: the role of titanian pargasite and kaersutite, J. Petrol. 42 (2001) 221–232.
[37] S. Klemme, J.D. Blundy, B.J. Wood, Experimental constraints on major and trace element partitioning during partial melting of eclogite, Geochim. Cosmochim. Acta 66 (2002) 3109–3123.
[38] K.H. Schmidt, P. Bottazzi, R. Vannucci, K. Mengel, Trace element partitioning between phlogopite, clinopyroxene and leucite lamproite melt, Earth Planet. Sci. Lett. 168 (1999) 287–299.
[39] S. Foley, M. Tiepolo, R. Vannucci, Growth of early continental crust controlled by melting of amphibolite in subduction zones, Nature 417 (2002) 837–840.
[40] C. Münker, G. Wörner, G. Yogodzinski, T. Churikova, Behaviour of high field strength elements in subduction zones: constraints from Kamchatka–Aleutian arc lavas, Earth Planet. Sci. Lett. 224 (2004) 275–293.
[41] K.W.W. Sims, D.J. DePaolo, Inferences about mantle magma sources from incompatible element concentration ratios in oceanic basalts, Geochim. Cosmochim. Acta 61 (1997) 765–784.
[42] M. Pertermann, M.M. Hirschmann, K. Hametner, D. Günther, M.W. Schmidt, Experimental determination of trace element partitioning between garnet and silica-rich liquid during anhydrous partial melting of MORB-like eclogite, Geochem. Geophys. Geosyst. 5 (2004) (Paper number 2003GC000638).
[43] M.M. Hirschmann, E.M. Stolper, A possible role for garnet pyroxenite in the origin of the "garnet signature" in MORB, Contrib. Mineral. Petrol. 124 (1996) 185–208.
[44] J. Phipps Morgan, W.J. Morgan, Two-stage melting and the geochemical evolution of the mantle: a recipe for mantle plum-pudding, Earth Planet. Sci. Lett. 170 (1999) 215–239.
[45] A. Stracke, V.J.M. Salters, K.W.W. Sims, Assessing the presence of garnet–pyroxenite in the mantle sources of basalts through combined hafnium–neodymium–thorium isotope systematics, Geochem. Geophys. Geosyst. 1 (1999) (Paper Number 1999GC000013).
[46] X.L. Xiong, T.J. Adam, T.H. Green, Rutile stability and rutile/melt HFSE partitioning during partial melting of hydrous basalt: implications for TTG genesis, Chem. Geol. 218 (2005) 339–359.
[47] M.W. Schmidt, A. Dardon, G. Chazot, R. Vannucci, The dependence of Nb and Ta rutile-melt partitioning on melt composition and Nb/Ta fractionation during subduction processes, Earth Planet. Sci. Lett. 226 (2004) 415–432.
[48] D. McKenzie, K.R. O'Nions, Partial Melt Distribution from Inversion of Rare Earth Element Concentrations, vol. 32, 1991, pp. 1021–1091.
[49] V.J.M. Salters, A. Stracke, Composition of the depleted mantle, Geochem. Geophys. Geosyst. 5 (2004) (Paper number 2003GC000597).
[50] R.K. Workman, S.R. Hart, Major and trace element composition of the depleted MORB mantle (DMM), Earth Planet. Sci. Lett. 231 (2005) 53–72.
[51] E.H. Hauri, T.P. Wagner, T.L. Grove, Experimental and natural partitioning of Th, U, Pb and other trace elements between garnet, clinopyroxene and basaltic melts, Chem. Geol. 117 (1994) 149–166.
[52] H. Becker, K.P. Jochum, R.W. Carlson, Trace element fractionation during dehydration of eclogites from high-pressure terranes and the implications for element fluxes in subduction zones, Chem. Geol. 163 (2000) 65–99.
[53] D. Rubatto, J. Hermann, Zircon formation during fluid circulation in eclogites (Monviso, Western Alps): implications for Zr and Hf budget in subduction zones, Geochim. Cosmochim. Acta 67 (2003) 2173–2187.
[54] R.L. Linnen, H. Keppler, Melt composition control of Zr/Hf fractionation in magmatic processes, Geochim. Cosmochim. Acta 66 (2002) 3293–3301.
[55] T. Zack, A. Kronz, S.F. Foley, T. Rivers, Trace element abundances in rutiles from eclogites and associated garnet mica schists, Chem. Geol. 184 (2002) 97–122.

[56] C. Chauvel, A.W. Hofmann, P. Vidal, HIMU-EM: the French–Polynesian connection, Earth Planet. Sci. Lett. 110 (1992) 99–119.
[57] T. John, E.E. Scherer, K. Haase, V. Schenk, Trace element fractionation during fluid-induced eclogitization in a subducting slab: trace element and Lu–Hf–Sm–Nd isotope systematics, Earth Planet. Sci. Lett. 227 (2004) 441–456.
[58] J. Patchett, J.D. Vervoort, U. Söderlund, V.J.M. Salters, Lu–Hf and Sm–Nd isotopic systematics in chondrites and their constraints on the Lu–Hf properties of the Earth, Earth Planet. Sci. Lett. 222 (2004) 29–41.
[59] K.P. Jochum, A. Stolz, G. McOrist, Niobium and tantalum in carbonaceous chondrites: constraints on the solar system and primitive mantle niobium/tantalum, zirconium/niobium, and niobium/uranium ratios, Meteorit. Planet. Sci. 35 (2000) 229–235.
[60] T. Kleine, K. Mezger, H. Palme, C. Münker, The W isotope evolution of the bulk silicate Earth: constraints on the timing and mechanisms of core formation and accretion, Earth Planet. Sci. Lett. 228 (2004) 109–123.
[61] J.L. Bodinier, F. Kalfoun, M. Godard, G. Barsczus, P. Sabate, Nb/Ta geochemical reservoirs, Geochim. Cosmochim. Acta 66 (2002) A85 (Spec. Suppl.).
[62] A. Stracke, M. Bizimis, V.J.M. Salters, Recycling oceanic crust: quantitative constraints, Geochem. Geophys. Geosyst. 4 (2003) (Paper number 2001GC000223).
[63] A. Scherstén, T. Elliott, C. Hawkesworth, M. Norman, Tungsten isotope evidence that mantle plumes contain no contribution from the Earth's core, Nature 427 (2004) 234–237.
[64] F. Albarède, J. Blichert-Toft, J.D. Vervoort, J.D. Gleason, M. Rosing, Hf–Nd isotope evidence for a transient dynamic regime in the early terrestrial mantle, Nature 404 (2000) 488–490.
[65] G. Caro, B. Bourdon, B.J. Wood, A. Corgne, Trace-element fractionation in Hadean mantle generated by melt segregation from a magma ocean, Nature 436 (2005) 246–249.
[66] G. Caro, B. Bourdon, J.L. Birck, S. Moorbath, Sm-146–Nd-142 evidence from Isua metamorphosed sediments for early differentiation of the Earth's mantle, Nature 423 (2003) 428–432.
[67] T.M. Harrison, J. Blichert-Toft, W. Müller, F. Albarède, P. Holden, S.J. Mojzsis, Heterogeneous Hadean hafnium: evidence of continental crust at 4.4 to 4.5 Ga, Science 310 (2005) 1947–1950.
[68] S.R. Hart, T. Dunn, Experimental cpx/melt partitioning of 24 trace elements, Contrib. Mineral. Petrol. 113 (1993) 1–8.
[69] K.T.M. Johnson, Experimental determination of partition coefficients for rare earth and high-field-strength elements between clinopyroxene, garnet, and basaltic melt at high pressure, Contrib. Mineral. Petrol. 133 (1998) 60–68.
[70] V.J.M. Salters, J. Longhi, Trace element partitioning during the inital stages of melting beneath mid-ocean ridges, Earth Planet. Sci. Lett. 166 (1999) 15–30.
[71] I. Horn, S.F. Foley, S.E. Jackson, G.A. Jenner, Experimentally determined partitioning of high-field strength-elements and selected transition-elements between spinel and basaltic melt, Chem. Geol. 117 (1994) 193–218.
[72] V.J.M. Salters, The generation of mid-ocean ridge basalts from the Hf and Nd isotope perspective, Earth Planet. Sci. Lett. 141 (1996) 109–123.
[73] S.R. Taylor, S.M. McLennan, The geochemical evolution of the continental crust, Rev. Geophys. 33 (1995) 241–265.
[74] J. Eisele, M. Sharma, S.J.G. Galer, J. Blichert-Toft, C.W. Devey, A.W. Hofmann, The role of sediment recycling in EM-1 inferred from Os, Pb, Hf, Nd, Sr isotope and trace element systematics of the Pitcairn hotspot, Earth Planet. Sci. Lett. 196 (2002) 197–212.
[75] C. Beier, A. Stracke, K.M. Haase, Evidence for enriched recycled oceanic crust in the mantle source of São Miguel (Azores), Earth Plant. Sci. Lett. (submitted for publication).
[76] R.K. Workman, S.R. Hart, M. Jackson, M. Regelous, K.A. Farley, J. Blusztajn, M. Kurz, H. Staudigel, Recycled metasomatized lithosphere as the origin of the enriched mantle II (EM2) end-member: evidence from the Samoan volcanic chain, Geochem. Geophys. Geosyst. 5 (2004) (Paper number 2003GC000623).
[77] J. Blichert-Toft, F.A. Frey, F. Albarède, Hf isotope evidence for pelagic sediments in the source of Hawaiian basalts, Science 285 (1999) 879–882.
[78] C. Chauvel, J. Blichert-Toft, A hafnium isotope and trace element perspective on melting of the depleted mantle, Earth Planet. Sci. Lett. 190 (2001) 137–151.